R. & M. No. 3412

MINISTRY OF AVIATION

AERONAUTICAL RESEARCH COUNCIL
REPORTS AND MEMORANDA

Transonic Compressor Noise
The Effect of Inlet Guide Vane/Rotor Spacing

By D. A. KILPATRICK and D. T. REID

LONDON: HER MAJESTY'S STATIONERY OFFICE
1965
PRICE 12*s.* 6*d.* NET

Transonic Compressor Noise
The Effect of Inlet Guide Vane/Rotor Spacing

By D. A. Kilpatrick and D. T. Reid

Communicated by the Deputy Controller Aircraft (Research and Development),
Ministry of Aviation

*Reports and Memoranda No. 3412**
January, 1964

Summary.

Comprehensive noise measurements were made in the inlet duct of a model of a typical two-stage transonic fan. The tests covered a range of variations in the inlet guide/rotor axial spacing from normal, in small increments, to a spacing of about one blade-chord length.

The effect of compressor speed and flow is pronounced for both the discrete blade tone and the vortex noise. As the axial spacing is increased the discrete blade tone output is reduced, the vortex noise being virtually unaffected.

LIST OF CONTENTS

* Replaces N.G.T.E. Report No. R.257—A.R.C. 25 641.

LIST OF APPENDICES

LIST OF ILLUSTRATIONS

---

1. *Introduction.*

With the advent of the ducted fan and the high by-pass ratio aircraft gas-turbine engine, the noise emanating from the compressor intake can no longer be neglected in comparison with the noise of the propulsive jet, particularly during the approach and landing manoeuvres.

This compressor noise has two characteristic parts—(i), discrete tones arising from the interaction of fixed and moving blades and (ii), vortex noise, a wide-band random noise resulting from the flow turbulence.

Although often lower in physical magnitude than the vortex component, the blade tones are disproportionately more important subjectively. Furthermore, although the magnitude of the vortex noise is reasonably understood in an empirical way (mainly for low speed, low-power fans and compressors), there is evidence to show that the blade tone output can vary widely for different compressor designs and operating conditions.

This report describes a set of detailed experiments on the effect of blade-row spacing on blade tone magnitude, and, as a by-product, further data on vortex noise are presented.

2. *Description of Test Rig.*

The experimental compressor is installed in the N.G.T.E. model transonic-compressor test rig, as shown in Fig. 1. The compressor is driven by an air turbine, the air supply being derived from a plant compressor facility nearby. Air is drawn into the test compressor through an intake, honeycomb, venturi meter, and various diffusing and settling lengths before the final contraction piece from 36 in. diameter down to the 12 in. diameter of the compressor face proper. Discharge from the compressor outlet to atmosphere is made *via* a radial diffuser, volute collector and outlet duct with throttle.

2.1. *Compressor.*

Ref. 1 gives full details of the design and performance of the two-stage transonic compressor, of which the following table briefly summarises the salient geometric features (*see* also Fig. 2). All blades are of two-arc profile and have a constant chord length of 1 in. The casing radius is constant at 6 in. and the rotor-blade tip clearances lie between 0·020 and 0·025 in. The normal mean diameter axial clearance between the inlet-guide-vane row (I.G.V.) and the first rotor row is 0·25 in., and incremental increases of 0·100 in. in this dimension are effected by the use of spacer rings as indicated in Fig. 2. There were nine available I.G.V./rotor axial spacing builds ranging from 0·25 in. to 1·05 in.

TABLE 1

Blade row	No. of blades	At rotor tip diameter (12 in.)		
		Thickness/chord per cent	Camber	Stagger
Inlet guide	20	10	36°	18°
1st Rotor	29	3	9°	−50°
1st Stator	42	10	31°	−28·5°
2nd Rotor	33	3	6°	−57°
2nd Stator	25	10	26°	−31°
Outlet guide	25	10	33°	− 8°

2.2. *Microphone Traverse.*

Measurements of the compressor noise were made in the 36 in. diameter duct immediately before the intake contraction. For reasons described later, it was considered essential to have a continuous radial traverse of the microphone. Fig. 3 shows the arrangement, the microphone being supported by a 5/8 in. diameter tube, which slides in self-lubricating P.T.F.E. plastic bushes in the duct walls. The radial movement of the microphone and tube is controlled by an electrically driven lead-screw. The limits of travel are from duct centre to 16 in. radius. It is also possible to make pre-set variations of up to 6 in. in the axial position of the microphone and tube.

2.3. *Duct Treatment.*

In order to minimise unwanted upstream sound reflections, the inside surface of the 36 in. diameter inlet duct (Figs. 1 and 3) was lined with Fibreglass, 1 in. thick, faced with scrim cloth under 22 s.w.g. perforated sheet ($13\frac{1}{2}$ per cent open face). Also fitted were cruciform-section splitters made of plywood, covered with Fibreglass $\frac{1}{2}$ in. thick, faced with 0·0015 in. thick P.V.C. plastic sheet, and held in place with 5/8 in. open-mesh wire netting.

The effect of the duct acoustic treatment was to reduce the reverberation time from 2·1 seconds (untreated) to 0·85 seconds (treated).

It may be of interest to note the failure of a first attempt to secure the 1 in. Fibreglass to the duct walls using open-mesh wire netting over 0·005 in. thick P.V.C. sheet, with circumferential steel retaining bands. The lining was pulled away from the wall, under running conditions, by the depression in the duct.

3. *Test Technique and Measurements.*

3.1. *Aerodynamic Measurements.*

These were as described in Ref. 1, with the exception that no inter-stage measurements were made. The overall pressure rise was derived from outlet static-pressure tappings and the inlet pitot, the temperature rise directly from thermocouples at inlet and outlet, and the mass flow by calibrated venturi readings.

The tests were made at four rotational speeds only and at each speed four or five settings of mass-flow condition were used. The nominal speeds were 18 000; 20 000; 22 000 and 23 000 rev/min (the design speed being 22 500 rev/min). The actual rotational speeds used (N rev/min) were adjusted for variations in the inlet absolute temperature (T°K). Constant values of $N/\sqrt{T}$ were thus maintained, N being exactly 18 000; 20 000 rev/min, etc. when T was 288°K. A stroboscopic device[2] was used to facilitate this type of speed setting, and great care was also taken that both hort- and long-time speed variations were minimised.

3.2. *Noise Measurements.*

A later report will describe the techniques of noise measurement and analysis. Only a brief outline is given here.

The microphone cartridge used was a 'Bruël and Kjaer' condenser type 4133 (0·5 in. diameter), affixed to its associated output impedance-matching cathode-follower unit. Connection was made *via* about 100 feet of cable with an equipment caravan outside the test cubicle. The microphone signal was fed to three selective amplifiers in parallel (Channels 1, 2 and 3), which can either be used 'flat' or as narrow-band frequency analysers (1/35 octave). Each analyser/amplifier has an associated level recorder—providing a chart record of the variations in r.m.s. level of the amplifier output. Channel 1 amplifier was used 'flat' to provide a continuous monitor of the overall Sound Pressure Level (S.P.L.), while Channels 2 and 3 respectively were tuned to the fundamental and first overtone blade-passing frequencies of the first-stage rotor (i.e. to $29E$ and $58E$ where E is the rotational frequency in rev/s, there being 29 rotor blades in the first stage). Simultaneous tape recordings were also made of the overall and the $29E$ component sound pressures, together with calibration and standard frequencies, speech, and marker pulses indicating microphone radial position. At each aerodynamic setting of the compressor, such recordings were made for the duration of the traverse of the microphone from the duct centre out to just beyond 16 in. radius, and for the return traverse. Before and after each traverse, outwards or inwards, electrical calibration signals were recorded.

4. *Method of Analysis.*

Typical traverse records of the overall and component S.P.L.'s are reproduced in Fig. 4, of which the most outstanding characteristic is the large variation with small changes in radius. As the records indicate, these variations are predominantly of the blade-passing tones. Any estimate of the acoustic power output or related property must therefore use an averaging process, taking account of these variations across the duct. The actual number of measurements made from the traverse records was limited to reduce the data reduction problem to reasonable proportions, samples being taken at 2 in. increments of radius, nine in all per traverse. Having converted the ordinates of the chart records, at the sampling points, into S.P.L. values (using the associated electrical calibrations and the transfer coefficient of the microphone), an average S.P.L. value ($\text{S.P.L.}_{\text{AV}}$) is calculated.

This S.P.L.$_{AV}$ is determined by assuming axial symmetry of the sound field in the duct, 'weighting' each sampled S.P.L. according to the annular area on which it is centred, and then averaging these weighted S.P.L.'s.

The acoustic power output from the compressor inlet (P.W.L.) is a simple function of the average S.P.L. and the duct area, since the acoustic treatment of the duct has been shown to reduce sound reflections from upstream of the measuring plane to small proportions.

5. *Data Reduction.*

The aerodynamic parameters of mass flow, pressure ratio, etc., were calculated in the conventional manner as indicated in Ref. 1, leading to the characteristics of Fig. 5.

As discussed earlier (Section 3.2) the noise information is recorded in two forms:

(i) continuous-trace chart records of the levels of the total (overall) noise and of its $29E$ and $58E$ components,

(ii) magnetic-tape recordings of the overall noise spectrum.

The sampling analysis of these 'on-line' chart records was done by using a manually controlled trace reader, with punched-tape output for final processing by digital computer. The computer output gave the S.P.L. at each sampling station, the average sound pressure level (S.P.L.$_{AV}$), and the acoustic power output (P.W.L.). Appendix I, by way of example, gives these values for one speed characteristic (five mass-flow conditions) for the three 'on-line' measured quantities. The 'cal. change' column gives the difference in measured values of the calibration levels before and after each traverse; ideally this should be zero but it should be noted that amongst other possible errors the resolution of the level recorders is only 0·5 dB.

To supplement and check the 'on-line' blade tone components, further spectrum analysis was performed using the tape recordings. Narrow-band (1/35 octave), 1/3 octave and octave band analysis was employed, depending on the part of the spectrum under scrutiny. For each band, chart records of the analyser output levels for the complete in and out traverses were made—similar to those produced 'on-line', and processed in exactly the same manner. This detailed analysis was applied to records at two speeds (one selected mass-flow condition at each speed) only, but at all I.G.V./rotor spacing configurations.

Even with this limitation (to about 10 per cent of the total test data) some 30 000 pieces of S.P.L. information were processed in the course of the spectrum analysis of the tape recordings, compared with approximately 10 000 for the total 'on-line' records.

6. *Performance of Measuring System.*

For a brief discussion it is convenient to divide the system into two parts, viz. the acoustic-mechanical and the electronic.

6.1. *Microphone.*

For a plane wave at normal incidence to its diaphragm, the microphone characteristic is reputed to be flat within $\pm$ 2 dB between 20 c/s and 40 kc/s. The upper frequency limit reduces with increasing departure from normal incidence of the sound. For sounds within $\pm$ 45° incidence, the response should be acceptably flat over the range including the fundamental and overtone first-stage rotor tones.

The self-noise and vibration response of the microphone were determined by two special tests, summarised in Fig. 6. By putting the microphone (facing downstream) in a 3 in. suction wind tunnel, a determination of the microphone self-noise, i.e. the apparent noise induced by the airflow over the microphone, was made. The air speed was 100 ft/s, being considerably higher than that obtaining in the compressor inlet duct. The octave band levels of the microphone signal are shown, the maximum level being in the band centred on 500 c/s. This maximum lies within the range of the Kármán vortex-shedding frequency as predicted empirically. A typical octave band spectrum of the signal from the microphone when traversed in the compressor duct is shown for comparison, and it is evident that the margin between 'signal' and 'self-noise' is satisfactory.

The vibration response of the microphone and cathode-follower unit was checked by traversing in the compressor duct with a blanking cap fitted to the microphone cartridge, in place of the normal protection grid. This virtually excludes direct impingement of the sound pressures on the diaphragm. The analysis of this test is also shown in Fig. 6, and it is seen that, apart from the lower bands, where electrical noise induced by the 50 c/s mains supply frequency and its harmonics is predominant, there is also a satisfactorily low vibration response.

6.2. *Electronics.*

Two principal arrangements of the system were used, namely the 'on-line' production of chart level records for overall S.P.L., $29E$ and $58E$ components, and the subsequent replaying of tape to produce complete spectrum records. The amplitude-frequency response of these system variants is shown in Fig. 7. The amplitude accuracy is estimated to be within $\pm$ 1·0 dB for overall S.P.L. and $29E$, $\pm$ 1·5 dB for the 1/3 octave and octave spectrum analysis, but possibly as much as $\pm$ 2·5 dB for the rest of the narrow-band analysis.

7. *Discussion of Test Results.*

The principal data reduced from the 'on-line' measurements are plotted, on a base of I.G.V./rotor spacing, in Figs. 8 to 11 and against the compressor flow coefficient*, V_a/u, in Figs. 13 to 16, whilst the more detailed spectrum analysis is given in Figs. 17 to 20. It will be convenient to discuss the various components separately.

7.1. *Overall Noise.*

Figs. 8 to 11 show the tendency for a minimum noise output to be observed as the I.G.V./rotor spacing approaches 1 in., whilst Figs. 13 to 16 show the general trend of decreasing noise with increasing V_a/u.

7.2. *First-Stage Rotor Tones.*

The variation of the fundamental ($29E$) and overtone ($58E$) rotor tone amplitudes with I.G.V./rotor spacing is seen from Figs. 8 to 11 to be quite significant (up to 5 dB) despite the large scatter, and in general reaches a minimum at spacings greater than 0·65 in. The overtone is approximately 5 dB down on the fundamental at 18 000 rev/min, but this separation increases to 10 dB or so at the higher speeds. The influence of flow parameter is demonstrated in Figs. 13 to 16, and, although showing no recognisable trend at 18 000 rev/min, is distinguished at the highest speed by a significant

---

* Based on mean diameter conditions, at inlet to the compressor.

reduction in acoustic power at the higher flows. The pressure-rise characteristics against flow coefficient are shown in Fig. 12, from which it may be observed that the attenuation at 23 000 rev/min at the highest flow is possibly associated with choking. In Ref. 1, dealing with the aerodynamic performance of this compressor design, it was thought likely that at high speeds the inlet guide vanes would be operating in excess of their critical Mach number, and thus be partially choked. The rotor itself has supersonic flow near the tips at this speed.

The bulk of the information on the first-stage rotor tones was obtained by analysis of the direct 'on-line' narrow-band records. Tape-record spectrum analysis, principally by 1/3 octave bands, of a limited number of records (Figs. 17 and 18) provides an analytical check. The $29E$ and $58E$ components do of course predominate in the relevant 1/3 octave bands, and these band readings are taken to be the tone amplitudes. The comparisons of the $29E$ and $58E$ tones as derived (1) from the 'on-line' narrow-band analysis (DIRECT) and (2) from the recorded spectrum 1/3 octave band analysis (PLAYBACK) are shown more clearly in Figs. 19 and 20, wherein the agreement between the two sets of $29E$ amplitudes is seen to be good—better than 1 dB on the average. The $58E$ comparisons show the 'direct' amplitudes to be consistently 2 to 3 dB lower than the playback derived ones. Since the frequency of the calibration signals is made exactly equal to the appropriate $29E$ frequency, the accuracy of measurement of the $29E$ component is expected to be good. The other components, particularly where narrow-band analysis is involved, will be determined less accurately —possibly only within $\pm$ 2·5 dB (*see* Section 6.2).

7.3. *Second-Stage Rotor Tones.*

It was not found possible to resolve sufficiently the fundamental ($33E$) and overtone ($66E$) components in the course of the 1/3 octave spectrum analysis, owing to their proximity to, and lesser stature than, the $29E$ and $58E$ (first-stage) components respectively. Consequently, narrow-band analysis was used to obtain the spectral lines at $33E$ and $66E$ in Figs. 17 and 18. From these it is seen that their amplitudes protrude some 30 dB above the general wide-band spectrum level in those regions. Figs. 19 and 20 show that there is no significant trend of $33E$ and $66E$ power level with changing I.G.V./rotor spacing, although there are comparatively large apparently random variations.

In general the second-stage fundamental rotor tone is larger than its overtone and is itself considerably lower than the first-stage fundamental rotor tone ($29E$) ranging from about 10 dB down at 18 000 rev/min to about 15 dB down at 22 000 rev/min.

Since, in the design of this two-stage compressor, each stage is similar and working under similar aerodynamic conditions, it is a reasonable assumption that each stage does equal work and generates equal noise. Making this assumption, the attenuation of the second-stage rotor blade tone, in passing through the first stage, is seen to be as much as 15 dB near the design speed.

7.4 *Other Spectral Lines.*

To investigate the increased levels observed for the octave bands centred on 125 and 250 c/s, a narrow-band analysis was made, which isolated components at 100 c/s, 150 c/s and the $1E$ frequency. These components are included in Figs. 17 to 20. The 100 and 150 c/s are of course electrical interference signals and there will undoubtedly also be a 50 c/s line component. That the $1E$ component is predominately derived from sound pressure fluctuations, rather than by mechanical interference, is shown in Fig. 6 (also Section 6), where the 'mechanical' response is at least 10 dB below the pressure response for a typical condition. This $1E$ component is presumably due to some asymmetry of flow; it shows a tendency to become a minimum at something like the same I.G.V./rotor spacing as does the first rotor tone component but is of comparatively low power, approximately 25 dB lower than the rotor tone. These other spectral line components (additional to the discrete blade tones) are all too low in amplitude to have any significant physical or subjective effect within the overall noise structure.

7.5. *Vortex Noise.*

By vortex noise is meant all the wide-band noise produced by vorticity, etc., generally within the compressor, as distinct from the discrete frequency components which are a result of the action and interaction between the wakes of the fixed and moving blades. Its spectrum is typified, therefore, in Figs. 17 and 18, by the continuous wide-band spectrum curves, with the line spectra excluded.

In estimating these vortex spectra, corrections have been made to the filter band readings to take account the 'splash-over' effect of the various discrete tones. As some of these corrections involve the difference of comparably large numbers, some error persists. The total vortex noise, being a function of the product of the individual spectrum levels and their associated bandwidths, is seen to be mainly contributed by the frequency range 500 c/s upwards. It will also be noted that there is a distinction between the shapes of the vortex spectra at 18 000 rev/min (Fig. 17) and at 22 000 rev/min (Fig. 18). At 18 000 rev/min there is almost a 10 dB rise and fall in spectrum level between 500 c/s and 30 000 c/s, peaking at 10 000 c/s. At 22 000 rev/min however, the tendency is for the spectrum level to remain constant between 500 c/s and 10 000 c/s, thereafter falling steadily (if the rapid fall* at 40 000 c/s is excluded). A possible explanation for the peak in the vortex spectrum levels in or about the 125 c/s octave band is that it is due to excitation by shed vortices from the microphone itself or its support tube. The mean frequency of vortex shedding is estimated to be about 160 c/s for these conditions, whereas for the 100 ft/s wind-tunnel experiment shown in Fig. 6 it was about 480 c/s—possibly accounting for the peak in the 500 c/s band in that figure.

In theory, the estimation of the total vortex noise is made (1) by the 'summation' of the individual vortex band levels or (2) by the 'subtraction' of all the discrete frequency components from the overall noise level. In practice the bulk of the vortex noise estimation has been made using the 'on-line' data, by the 'subtraction' of the $29E$ and $58E$ components *only* from the overall noise levels. That this neglect of all the other discrete components is not significantly inaccurate is shown by analysing the results of Figs. 17 and 18. The following table shows the comparison between the vortex noise calculated by the 'summation' (1) above, next by subtracting $29E$, $33E$, $58E$ and $66E$ from the overall noise, and finally by subtracting $29E$ and $58E$ only from the overall noise. The accuracy of estimating the vortex noise from 'OVERALL $-$ ($29E + 58E$)' is thus seen to be acceptable.

The principal overall vortex noise characteristics are given in Figs. 8 to 11 and 13 to 16. There is seen to be no effective dependence of the power levels on I.G.V./rotor spacing, but a quite definite tendency for vortex noise to increase with decreasing flow parameter, i.e. towards stall.

* This phenomenon is not reproduced in 18 000 rev/min analysis since, there, the highest frequency range was covered by an octave filter, centred on 31 500 c/s, whereas for Fig. 18 the higher frequencies of the tones necessitated the use of 1/3 octave filters, the top one being centred on 40 000 c/s. The decay in power at these high frequencies is in some part due to the falling microphone and amplifier responses.

TABLE 2

I.G.V./rotor spacing in.	Vortex Noise					
	By 'summation'	Overall—(29E+33E+58E+66E)	Overall—(29E+58E)	By 'summation'	Overall—(29E+33E+58E+66E)	Overall—(29E+58E)
0·25	139·24	138·19	139·32	135·56	138·59	138·95
0·35	140·15	140·40	140·98	135·60	130·68	132·07
0·45	140·52	140·58	140·95	137·16	138·65	138·92
0·55	140·11	140·72	141·31	136·89	137·64	138·33
0·65	139·84	141·03	141·65	135·78	136·67	137·26
0·75	139·05	141·51	141·87	137·59	137·02	137·16
0·85	139·50	139·45	140·15	136·31	135·31	135·89
0·95	140·29	140·71	141·19			
1·05	141·55	141·93	142·39	138·56	137·43	138·06
Compressor condition	18 000 rev/min $V_a/u = 0\cdot57$			22 000 rev/min $V_a/u = 0\cdot61$		

Correlation has also been attempted with formulae empirically derived from ventilation fan testing, as given for example in Ref. 3. A reduced form of these formulae is as follows:

$$\text{P.W.L.} = 97 + 10 \log \text{h.p.} + 10 \log \Delta T$$

where

P.W.L. is noise power output from either end of fan in dB re 10^{-12} watts,

h.p. = fan horsepower,

and

ΔT = fan temperature rise, C deg.

The measured vortex noise levels, relative to the values obtained by calculation using the above formula, are plotted in Figs. 8 to 11. Confined to a consideration of conditions near the compressor's usual working point (i.e. for $V_a/u = 0\cdot6$ approximately) the correlation is seen to range from $+2/-1$ dB at 18 000 rev/min to $-5/-7$ dB at 23 000 rev/min.

In applying the formula it is assumed that the vortex noise output of stage 2 is attenuated to insignificant proportions in passing through to the inlet duct, and that the horsepower and temperature rise are those of the first stage only. In the absence of stage measurements these are taken as half the overall (two-stage) quantities. The correlation (for optimum flow parameter) at the lower speeds is thus seen to be good. As the compressor speed rises, i.e. as the air velocities within the compressor rise, the empirical rule increasingly overestimates the vortex noise—by about 6 dB at the highest speed.

8. *Repeat Tests.*

The data presented so far are from a complete series of tests embracing all the various configurations of I.G.V./rotor axial spacing. Subsequently, selected configurations were re-tested and the 'on-line' recorded data analysed. This is presented as Appendix II, being tabulated for comparison with the original test results for the same configurations. Generally speaking, the repeat tests gave slightly lower values, the mean values and standard deviations (based on 58 measurements for each component) being tabulated below.

TABLE 3

Component	Mean repeat P.W.L.'s, dB re original values	Standard deviation, dB
Overall	−1·44	1·09
29*E*	−1·76	1·44
58*E*	−0·53	1·75

These are acceptable values in this context and none of the trends or general results noted previously would be affected by such scatter.

9. *An Apparently Anomalous Result.*

During the original series of tests, measurements at an I.G.V./rotor spacing of 0·75 in. were first made with the 'on-line' chart recordings only, at 18 000 rev/min and 22 000 rev/min. Within a few days, without any disturbance, this build was re-tested with the tape-recording system operational. Analyses showed that, at the 18 000 rev/min condition the blade tone components were significantly lower, about 8 dB, for the original test; while at 22 000 rev/min the amplitudes were comparable for the two tests. At the end of the complete series of I.G.V./rotor-spacing tests, repeat tests were made paying particular attention to this configuration. Fig. 21 reviews these measurements and it is seen that the repeat tests did not reproduce the first low values of blade tones. No simple theory of experimental error can be advanced, since all three channels are subject to common calibration signals and the repeatability of the overall noise is apparent. The vortex noise, omitted from Fig. 21 for clarity, also gave very repeatable results.

The anomaly was particularly intriguing since the parameter I.G.V./rotor axial spacing was almost exactly equal to half the wavelength of the blade tone at 18 000 rev/min, thus suggesting some partial-cancellation phenomenon. If such were the case the effect would be critically dependent on blade tone frequency, so tests were run with the microphones successively at two fixed positions while the compressor speed was slowly varied between 17 000 and 19 000 rev/min and back again. These results are shown in the lower graphs of Fig. 21 and, although there is a considerable variation of the S.P.L. between acceleration and deceleration for the 8 in. microphone position, there is no consistent indication of a large attenuation of blade tone as its frequency varies.

In view of all the experimental evidence, it is believed that this is a true anomaly rather than a reflection of experimental error.

10. *Conclusions.*

A comprehensive series of tests has been performed, on a 12 in. diameter model compressor, primarily to investigate the effects of varying the I.G.V./rotor axial spacing on the compressor noise output. The following is a summary of the results.

10.1 *Effect of I.G.V./Rotor Axial Spacing.*

(a) The first-stage rotor-blade fundamental tone is reduced by approximately 5 dB as the axial spacing approaches 1 in.

(b) The vortex noise is virtually unaffected.

10.2. *Effect of Compressor Flow Parameter, V_a/u.*

(a) The first-stage blade tone tends to be unaffected at the lowest speed, but to be attenuated as V_a/u increases at the higher speeds.

(b) The vortex noise is continuously dependent on V_a/u, and increases as V_a/u decreases, i.e. as the incidence of the air to the blading increases.

(c) At the highest speed choking was approached, resulting in the apparent beginnings of large attenuation of both tone and vortex noise.

10.3 *Effect of Compressor Speed.*

With V_a/u held approximately constant, neither blade tone nor vortex noise shows much tendency to alter with speed. This is contrary to the evidence for fans and compressors at lower speeds, where a rapid increase of noise with speed is observed.

However, the speed range of these tests is comparatively small, and even at the lowest speed there are locally supersonic flows. The lack of significant increase of noise with increasing speed may therefore be due to the increasing extent of these flows.

At the design flow parameter at the lowest speed, the vortex noise agrees well with estimates using fan noise formulae. At the higher speed, the vortex noise is about 6 dB lower than the estimates.

10.4. *Second-Stage Rotor-Blade Fundamental Tone.*

This is not significantly affected by changes in I.G.V./rotor axial spacing. The tone amplitude appears to be attenuated by as much as 15 dB in passing through the first stage.

REFERENCES

No.	*Author(s)*	*Title, etc.*
1	R. Staniforth and I. M. Davidson	The performance of a two-stage transonic fan. N.G.T.E. Memo. M.345. A.R.C. 22 875. February, 1961.
2	N. A. Dimmock	A compressor routine test code. A.R.C. R. & M. 3337. January, 1961.
3	L. L. Beranek	*Noise reduction.* p. 545, McGraw-Hill. 1960.

APPENDIX I

Sample of Reduced Data for I.G.V./Rotor Spacing = 0·65

Nom. speed	Run No.	Component	Dirn. of Trav.	SPL_R									SPL_{AV}	P.W.L.	Cal. Change dB
				$R = 0$	2 in.	4 in.	6 in.	8 in.	10 in.	12 in.	14 in.	16 in.			
18 000	1	O.A.S.P.L.	OUT	134·00	135·29	134·93	136·17	134·72	136·07	136·33	136·33	134·47	135·65	133·14	−0·10
	1		IN	134·05	135·19	135·08	136·38	134·88	137·00	135·81	136·48	135·29	135·93	133·43	+0·00
	2		OUT	131·30	132·02	132·08	134·00	132·80	132·65	133·84	134·42	132·34	133·28	130·78	−0·16
	2		IN	131·04	131·82	131·72	134·00	132·44	133·07	133·53	134·42	132·03	133·17	130·67	−0·10
	3		OUT	131·04	139·93	131·56	132·02	133·01	132·75	133·84	134·68	132·44	133·21	130·70	+0·05
	3		IN	130·47	132·03	131·46	131·61	132·75	132·13	133·48	134·88	133·22	133·25	130·74	−0·05
	4		OUT	129·63	131·30	131·45	131·71	131·30	133·95	131·71	133·27	132·23	132·46	129·96	−0·05
	4		IN	130·31	131·56	131·40	131·77	131·14	133·48	131·04	133·64	132·28	132·38	129·88	−0·10
	5		OUT	130·15	130·10	130·36	131·66	132·86	133·38	130·88	131·19	132·86	132·08	129·58	+0·00
	5		IN	130·77	130·20	130·46	131·66	132·96	132·44	131·35	131·81	132·44	132·01	129·50	+0·05
18 000	1	29*E*	OUT	122·46	127·97	125·16	130·52	123·66	129·79	127·66	130·73	129·43	129·07	126·57	+0·21
	1		IN	122·43	127·46	125·44	129·18	124·77	132·13	127·52	130·42	128·76	129·23	126·73	−0·36
	2		OUT	120·50	123·31	119·61	127·48	122·32	126·02	127·01	129·78	128·73	127·52	125·02	+0·16
	2		IN	120·27	123·04	119·54	126·75	121·68	125·81	126·95	129·88	128·26	127·31	124·81	+0·05
	3		OUT	124·53	125·47	127·13	122·71	123·33	127·13	129·89	130·25	129·11	128·44	125·94	+0·05
	3		IN	124·36	127·59	128·22	120·77	122·28	126·66	129·57	130·56	129·99	128·68	126·18	+0·05
	4		OUT	122·52	127·16	127·79	123·61	125·60	130·50	127·01	129·56	130·50	128·87	126·36	+0·05
	4		IN	122·66	128·17	128·17	124·22	125·73	130·41	126·30	129·53	130·46	128·82	126·31	+0·21
	5		OUT	125·41	125·15	124·00	126·81	129·73	129·16	126·14	127·96	130·41	128·54	126·04	+0·05
	5		IN	126·40	126·14	124·21	127·28	129·73	129·47	126·60	127·33	130·30	128·55	126·05	+0·10
18 000	1	58*E*	OUT	123·55	125·06	125·58	125·22	123·24	125·79	129·58	128·44	124·85	126·87	124·37	+0·16
	1		IN	123·11	124·66	126·22	123·94	122·54	124·66	127·36	127·31	124·04	125·61	123·11	−0·99
	2		OUT	120·17	119·86	123·30	123·67	122·67	121·84	124·76	125·18	119·54	123·21	120·71	+0·21
	2		IN	120·25	119·68	121·55	124·00	122·65	120·72	124·78	125·61	121·08	123·37	120·87	−0·05
	3		OUT	120·32	120·42	120·52	122·35	123·59	121·20	122·97	122·61	119·28	121·89	119·39	−0·42
	3		IN	119·80	120·43	120·38	122·05	123·25	120·80	123·35	122·67	115·32	121·53	119·02	+0·26
	4		OUT	117·99	118·41	120·13	121·23	120·29	123·10	120·91	120·24	116·69	120·42	117·92	−0·36
	4		IN	119·12	118·86	121·04	121·62	120·52	124·06	120·94	121·25	115·69	120·93	118·43	+0·47
	5		OUT	118·29	118·50	121·42	118·60	120·22	119·49	122·62	119·59	114·79	119·76	117·25	−0·42
	5		IN	118·67	117·58	121·37	118·93	120·85	120·12	124·33	120·59	115·13	120·72	118·22	+0·73

Note.—SPL_R, SPL_{AV} in dB re 0·0002 dynes/cm^2. P.W.L. in dB re 10^{-12} watts.

APPENDIX II

Repeatability Measurements

Speed 18 000 rev/min	Nominal V_a/u	I.G.V./rotor spacing (in.)	Original P.W.L. (dB re 10^{-12} W)	Repeat P.W.L.'s – original P.W.L.
Overall noise	0·57	0·45	135·73	−1·59, −1·34, −0·88, −0·74
	0·61	0·65	131·78	−2·22
	0·65	0·65	131·70	−1·41
	0·57	0·75	134·48	−2·52, −2·53, −1·11, −1·03, +0·66, +0·56
	0·61	0·75	131·88	−2·14
	0·65	0·75	131·72	+1·67
	0·68	0·75	131·69	−2·28, −2·24
	0·70	0·75	131·38	−2·10
	0·57	0·95	133·83	+0·41
	0·65	0·95	131·72	−4·18
	0·57	1·05	135·00	−3·63
	0·61	1·05	133·37	−3·03
	0·65	1·05	132·27	−2·87
	0·68	1·05	131·28	−2·10
	0·70	1·05	131·30	−2·60
Blade tone, fundamental 29*E*	0·57	0·45	130·86	−5·88, −5·16, −3·92, −3·70
	0·61	0·65	126·01	−1·85
	0·65	0·65	126·95	−1·00
	0·57	0·75	128·92	−0·80, −1·51, −2·88, −1·78, −2·21, −1·98
	0·61	0·75	124·70	−1·24
	0·65	0·75	128·57	−2·28
	0·68	0·75	128·72	−3·07, −2·05
	0·70	0·75	128·24	−1·61
	0·57	0·95	126·51	−0·17
	0·65	0·95	126·84	−1·80
	0·57	1·05	128·21	−2·80
	0·61	1·05	128·25	−2·39
	0·65	1·05	127·36	−1·95
	0·68	1·05	125·33	−1·06
	0·70	1·05	126·98	−1·24
Blade tone, 1st overtone 58*E*	0·57	0·45	125·49	+1·98, +1·98, +1·86, +1·66
	0·61	0·65	121·70	+0·28
	0·65	0·65	120·38	+0·64
	0·57	0·75	126·23	+2·05, +0·55, −0·40, −0·17, +0·16, −0·03
	0·61	0·75	123·70	+0·36
	0·65	0·75	122·35	−0·23
	0·68	0·75	120·23	+0·80, +0·36
	0·70	0·75	118·75	+1·90
	0·57	0·95	124·03	+1·50
	0·65	0·95	120·03	+2·02
	0·57	1·05	124·37	−0·44
	0·61	1·05	121·82	+0·29
	0·65	1·05	123·43	−3·37
	0·68	1·05	121·31	−0·88
	0·70	1·05	120·89	−3·07

APPENDIX II—*continued*

Speed 20 000 rev/min	Nominal V_a/u	I.G.V./rotor spacing (in.)	Original P.W.L. (dB re 10^{-12} W)	Repeat P.W.L.'s – original P.W.L.
Overall noise	0·64	0·65	130·88	−0·55
	0·71	0·65	128·06	−0·35
	0·64	0·75	130·81	−0·37
	0·71	0·75	127·95	−1·49
	0·64	0·95	130·37	−0·42
	0·71	0·95	129·10	−2·62
	0·59	1·05	134·06	−1·15
	0·64	1·05	132·10	−1·55
	0·68	1·05	131·62	−2·45
	0·71	1·05	130·50	−1·98
	0·74	1·05	128·40	−0·59
Blade tone, fundamental 29*E*	0·64	0·65	126·53	+1·33
	0·71	0·65	126·73	−0·74
	0·64	0·75	126·91	−1·04
	0·71	0·75	123·44	+0·25
	0·64	0·95	125·92	+1·02
	0·71	0·95	124·32	−2·35
	0·59	1·05	130·33	−2·21
	0·64	1·05	126·63	+0·12
	0·68	1·05	127·57	−2·11
	0·71	1·05	126·38	−2·45
	0·74	1·05	123·71	+0·06
Blade tone, 1st overtone 58*E*	0·64	0·65	121·79	−1·37
	0·71	0·65	116·35	−1·00
	0·64	0·75	117·78	+2·12
	0·71	0·75	113·42	+2·82
	0·64	0·95	118·15	+1·77
	0·71	0·95	115·99	0·00
	0·59	1·05	123·65	−1·98
	0·64	1·05	120·52	−1·66
	0·68	1·05	116·98	−0·28
	0·71	1·05	117·69	−2·04
	0·74	1·05	116·26	−1·96

APPENDIX II—*continued*

Speed 22 000 rev/min	Nominal V_a/u	I.G.V./rotor spacing (in.)	Original P.W.L. (dB re 10^{-12} W)	Repeat P.W.L.'s – original P.W.L.
Overall noise	0·61	0·45	133·91	−1·06, −1·66
	0·61	0·65	132·91	+0·86
	0·73	0·65	129·58	−0·69
	0·61	0·75	133·46	−2·56, −0·20, −0·13
	0·67	0·75	130·84	−0·43
	0·71	0·75	130·40	−1·37
	0·71	0·95	128·67	−1·83
	0·73	0·95	127·93	−1·43
	0·61	1·05	134·70	−2·22
	0·67	1·05	130·84	−2·29
	0·71	1·05	129·02	−2·34
	0·73	1·05	128·37	−1·75
Blade tone, fundamental 29*E*	0·61	0·45	129·83	−4·95, −3·40
	0·61	0·65	127·43	−1·44
	0·73	0·65	127·22	−1·98
	0·61	0·75	129·72	−2·31, −2·77, −2·20
	0·67	0·75	127·66	−0·71
	0·71	0·75	128·36	−1·54
	0·71	0·95	126·21	−1·43
	0·73	0·95	124·48	−0·77
	0·61	1·05	130·71	−3·08
	0·67	1·05	127·73	−2·93
	0·71	1·05	123·11	+0·15
	0·73	1·05	122·60	+0·69
Blade tone, 1st overtone 58*E*	0·61	0·45	123·24	−5·67, −3·64
	0·61	0·65	121·86	−2·13
	0·73	0·65	115·66	+0·99
	0·61	0·75	120·58	−0·25, −1·85, −1·91
	0·67	0·75	118·47	−0·63
	0·71	0·75	115·57	+0·20
	0·71	0·95	114·35	−1·32
	0·73	0·95	112·84	−1·93
	0·61	1·05	121·73	−2·89
	0·67	1·05	116·49	−0·62
	0·71	1·05	114·66	−2·89
	0·73	1·05	113·03	−2·19

Speed 23 000 rev/min	Nominal V_a/u	I.G.V./rotor spacing (in.)	Original P.W.L. (dB re 10^{-12} W)	Repeat P.W.L.'s – original P.W.L.
Overall noise	0·61	0·65	133·78	−1·43
	0·71	0·65	130·61	−1·30
	0·71	0·75	130·46	−1·44, −1·09
	0·61	0·95	134·56	−1·44
	0·69	0·95	131·79	+0·10
	0·61	1·05	134·55	−2·72
	0·69	1·05	131·71	−2·48
Blade tone, fundamental 29*E*	0·61	0·65	130·42	−1·99
	0·71	0·65	128·20	−1·92
	0·71	0·75	128·06	−1·92, −1·05
	0·61	0·95	130·33	−0·83
	0·69	0·95	129·08	+0·84
	0·61	1·05	129·67	−0·70
	0·69	1·05	129·65	−3·35
Blade tone, 1st overtone 58*E*	0·61	0·65	117·06	+1·55
	0·71	0·65	114·39	+0·70
	0·71	0·75	123·52	−0·90, −3·98
	0·61	0·95	131·53	−1·35
	0·69	0·95	127·98	−0·94
	0·61	1·05	131·48	−2·56
	0·69	1·05	127·64	−2·49

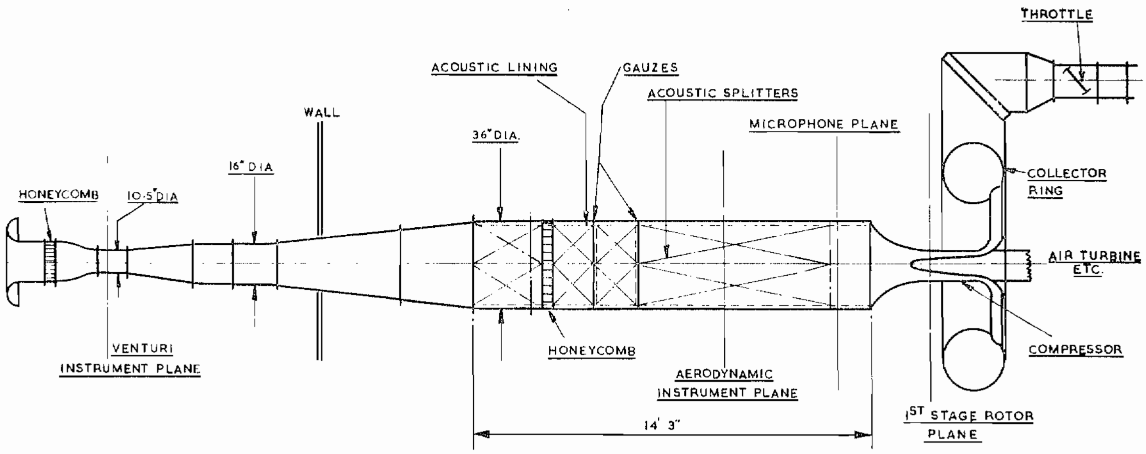

Fig. 1. Compressor noise test rig.

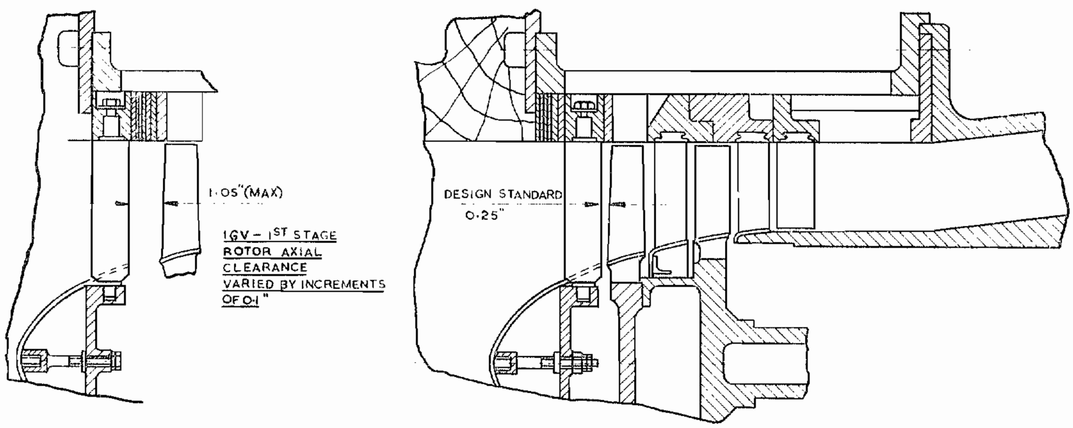

Fig. 2. Layout of compressor in test rig.

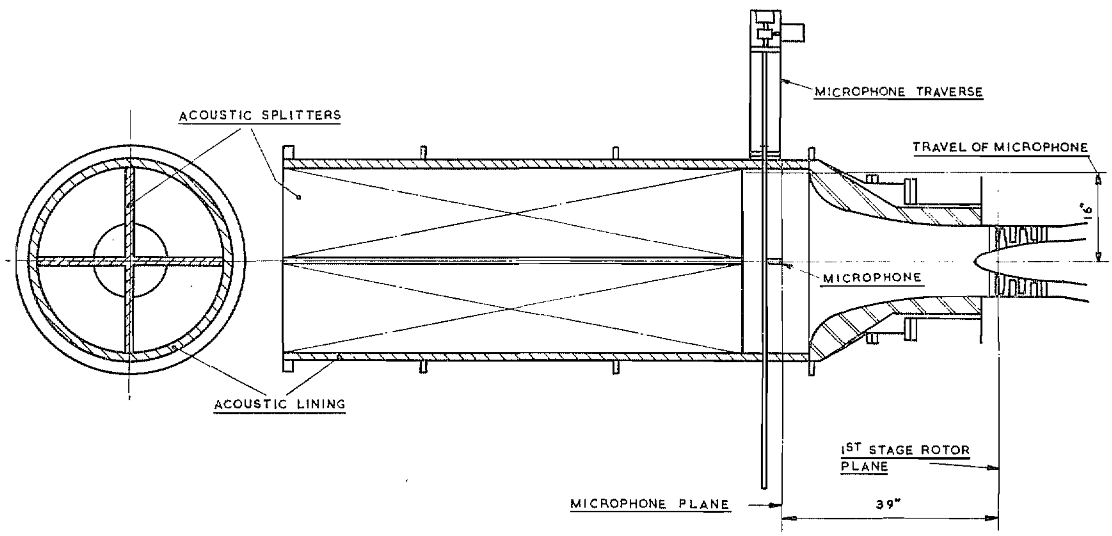

FIG. 3. Arrangement of microphone in duct. Compressor noise test rig.

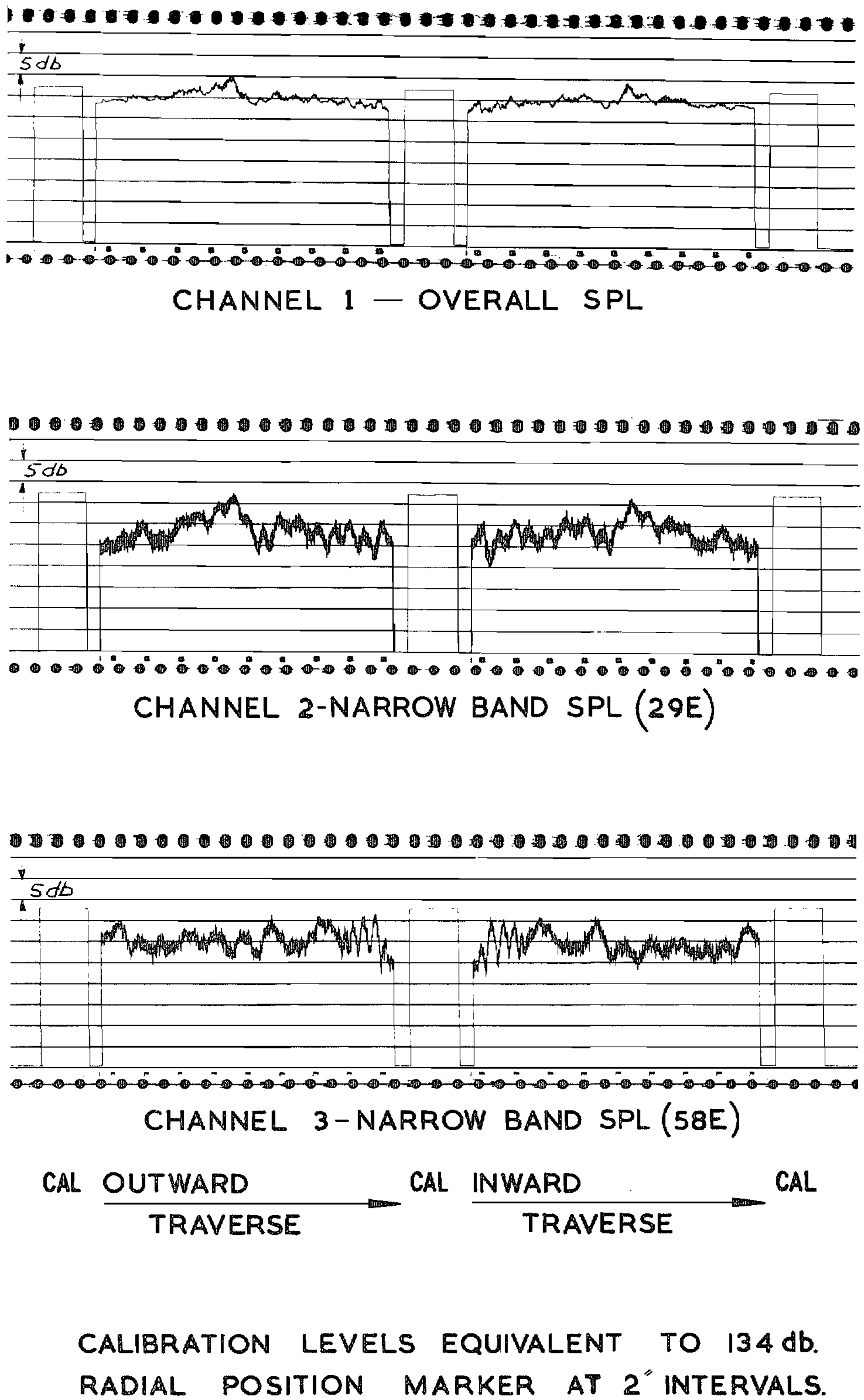

FIG. 4. Typical microphone traverse records.

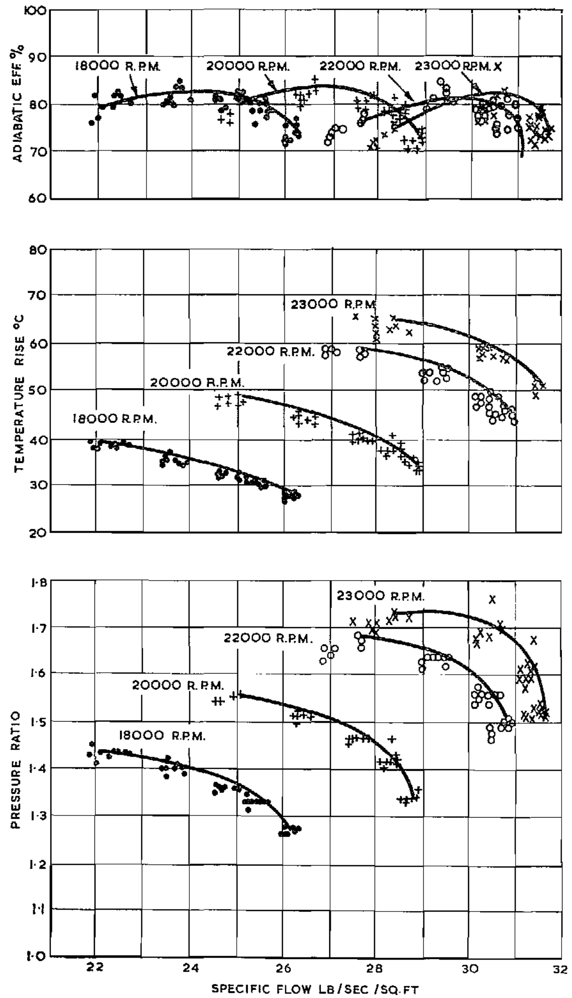

(NOTE :- FULL LINES REFER TO IGV - ROTORSPACING = 0·25"
OTHER POINTS FROM TESTS AT INCREASED SPACINGS)

FIG. 5. Performance of compressor.

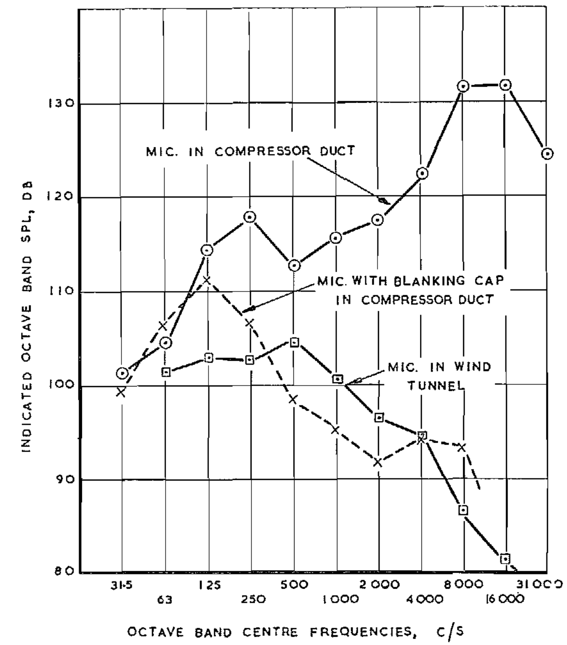

COMPRESSOR CONDITIONS :- 20 000 R.P.M., BLADE TONES AND OVERTONES LIE IN OCTAVE BANDS 8 000, 16 000, 31 500 C/S, VELOCITY IN INLET DUCT 40 FT/S APPROX. SIGNAL ANALYSIS MADE FROM TAPE RECORDINGS.

WIND TUNNEL CONDITIONS:- SUCTION TYPE TUNNEL, 100 FT/S AIR VELOCITY SIGNAL ANALYSIS MADE 'ON-LINE'.

FIG. 6. Interference signal characteristics of microphone system.

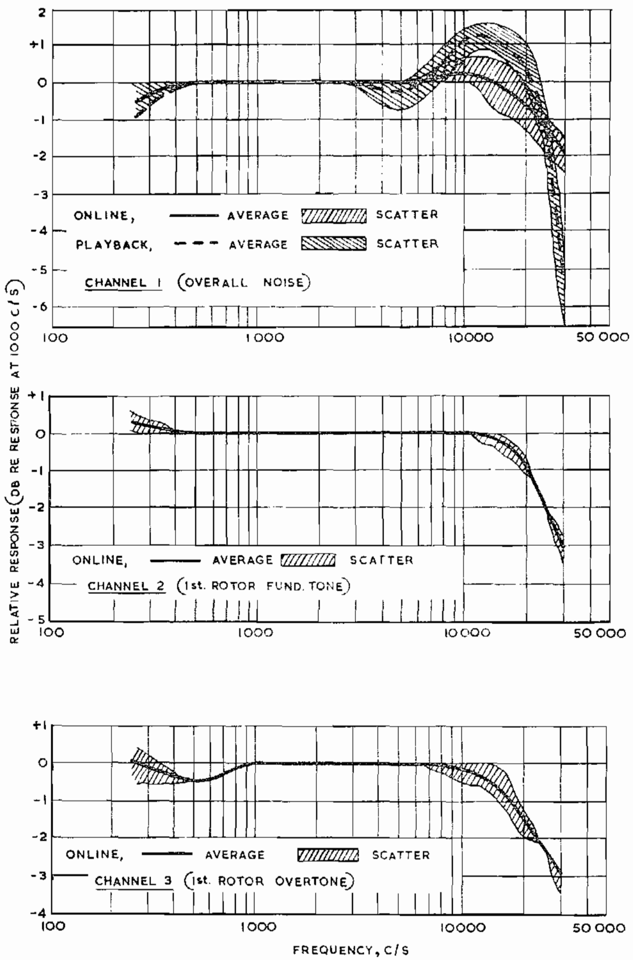

FIG. 7. Frequency response of electrical system.

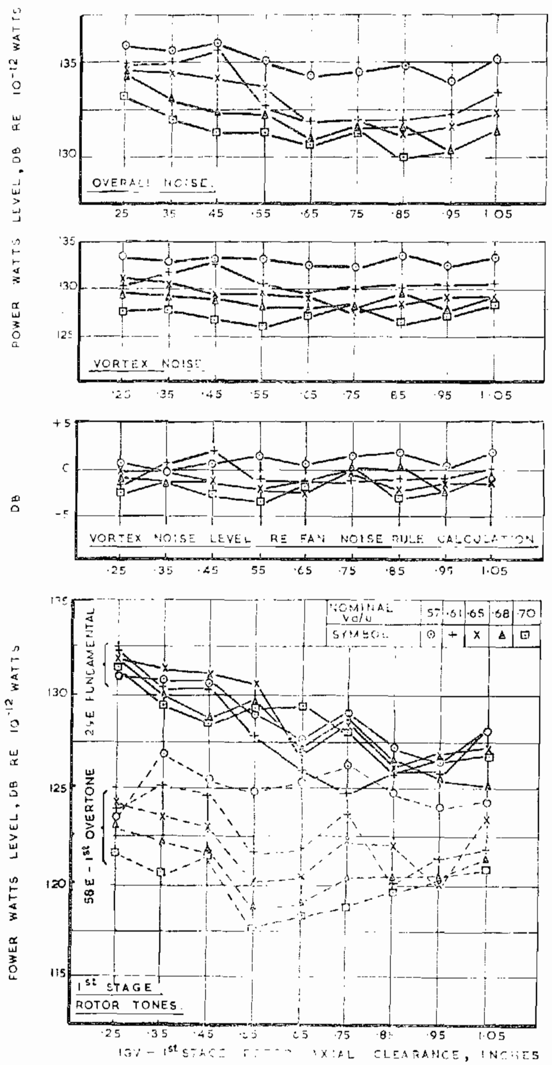

FIG. 8. Noise levels—18 000 rev/min.

(91595)

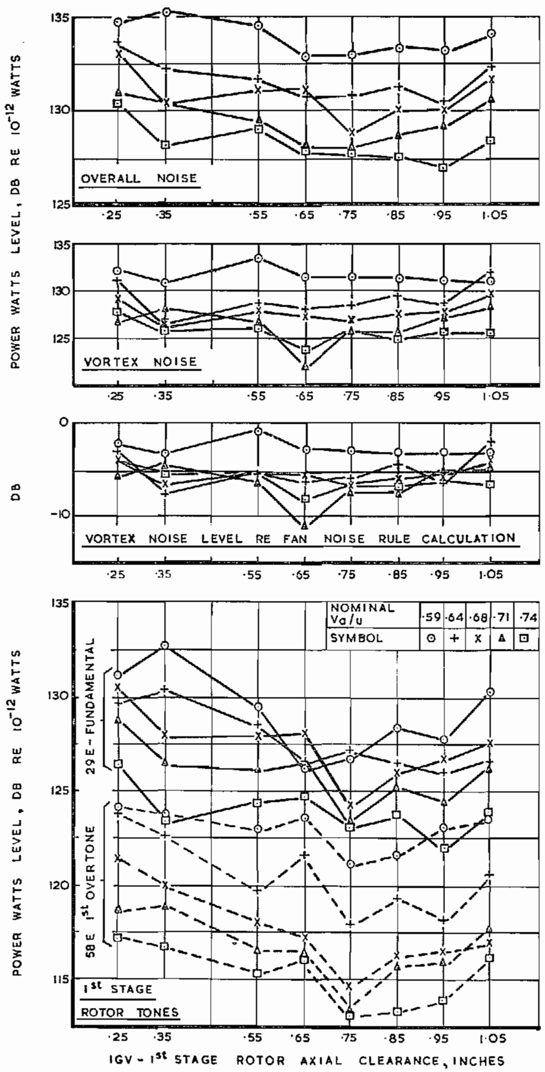

FIG. 9. Noise levels—20 000 rev/min.

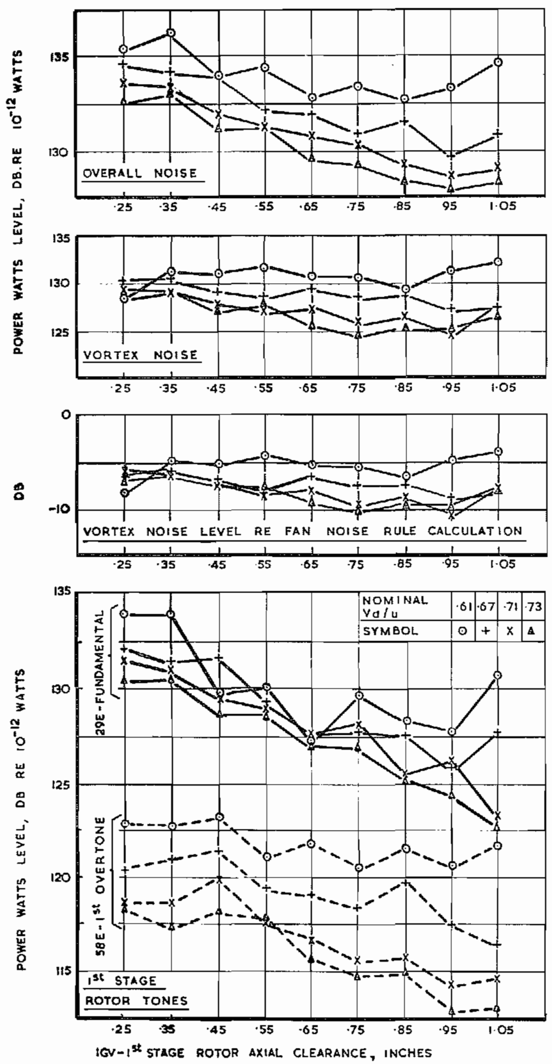

FIG. 10. Noise levels—22 000 rev/min.

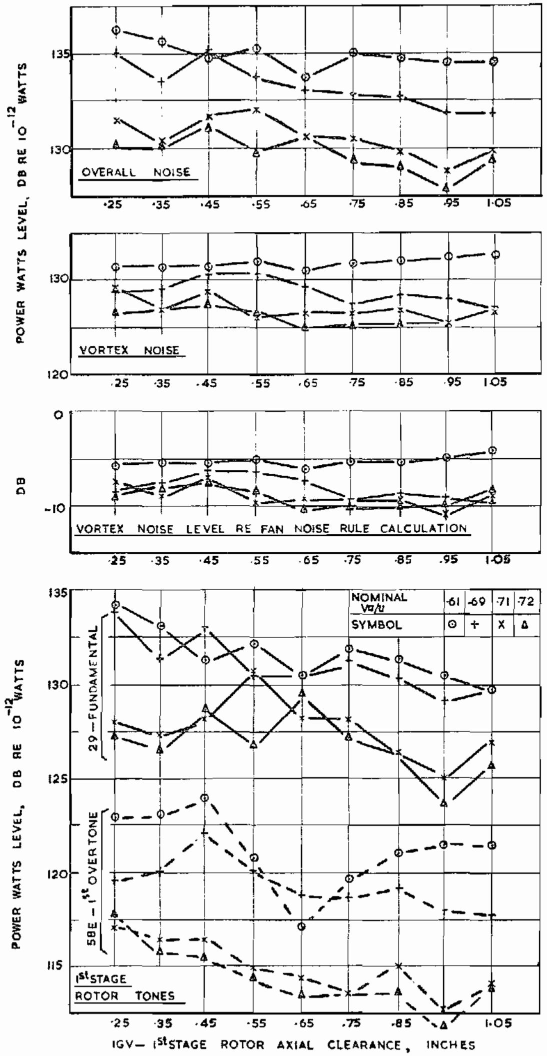

FIG. 11. Noise levels—23 000 rev/min.

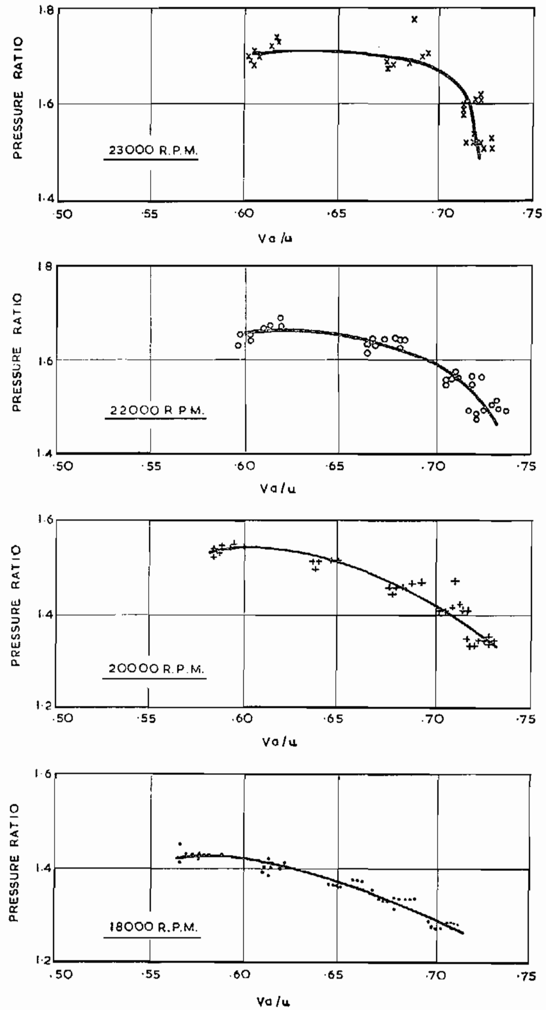

FIG. 12. Pressure ratio versus V_a/u.

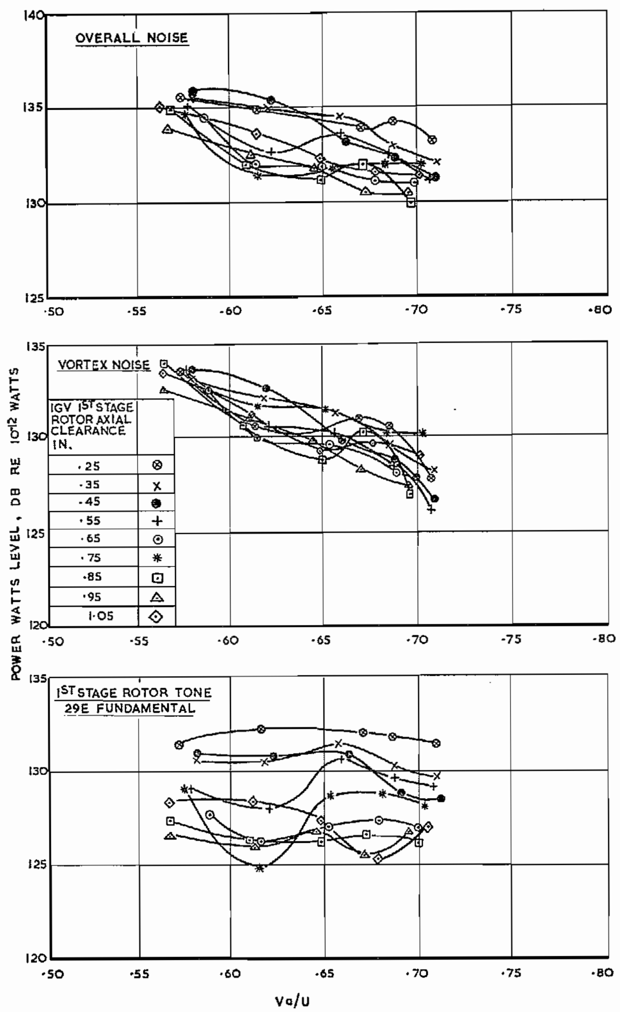

FIG. 13. 18 000 rev/min—noise levels *versus* V_a/u.

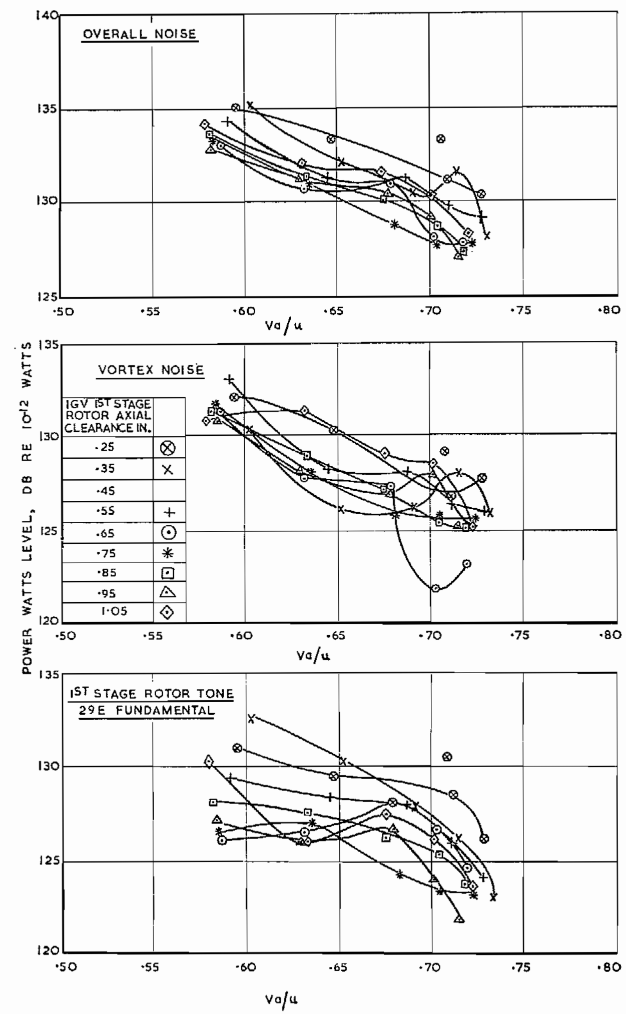

FIG. 14. 20 000 rev/min—noise levels *versus* V_a/u.

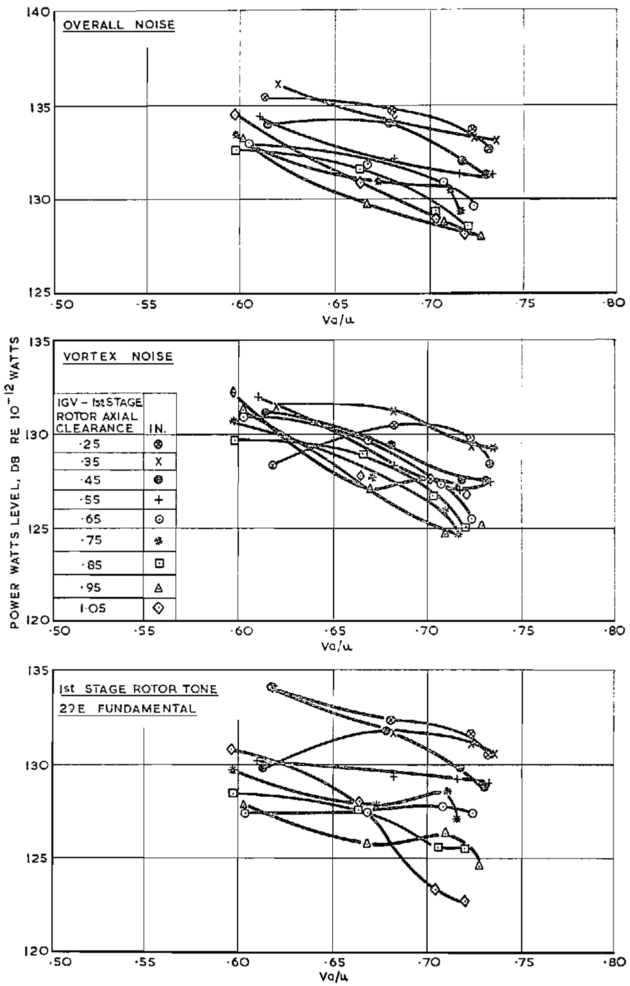

FIG. 15. 22 000 rev/min—noise levels *versus* V_a/u.

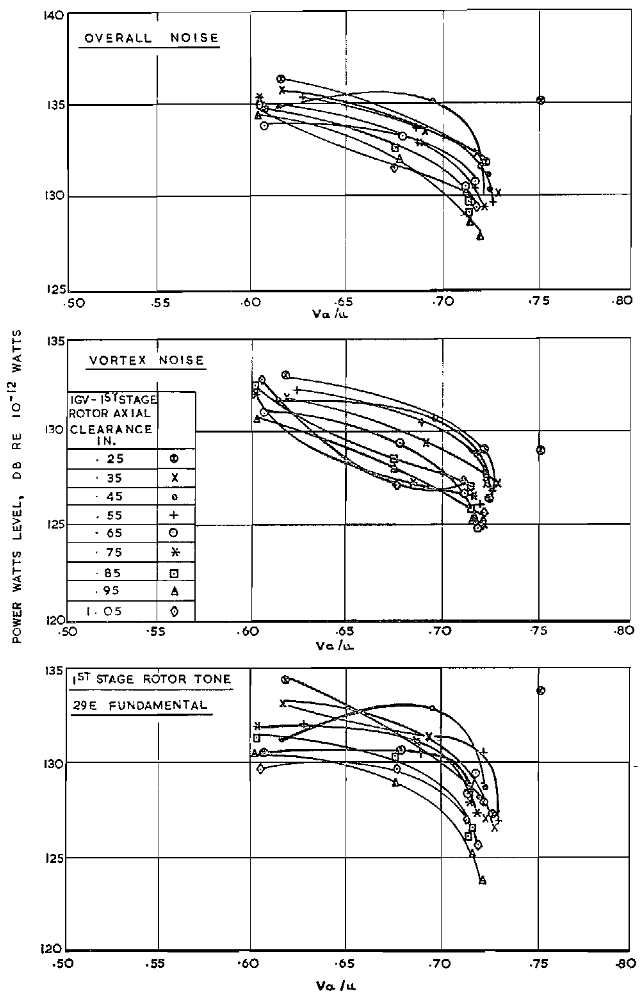

FIG. 16. 23 000 rev/min—noise levels *versus* V_a/u.

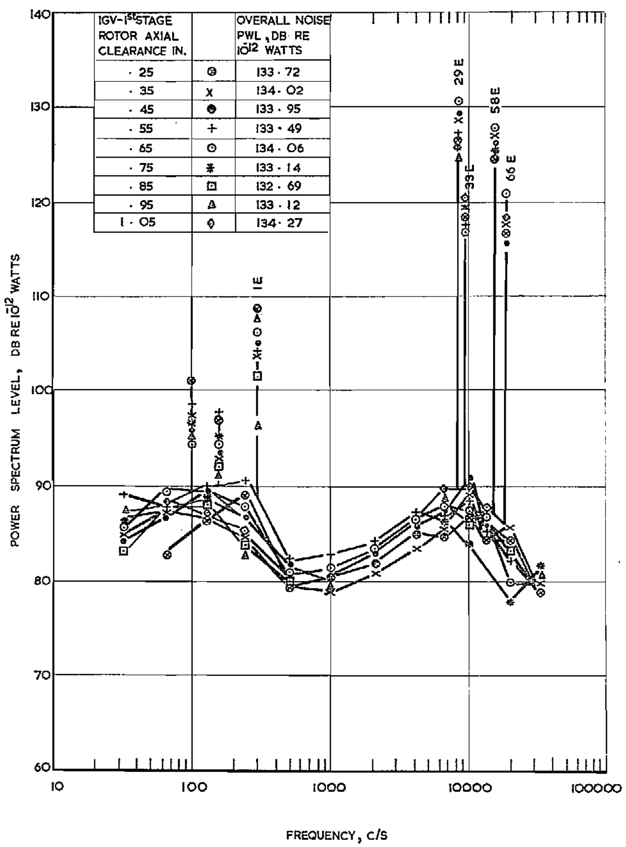

FIG. 17. Frequency spectrum—18 000 rev/min. $V_a/u = 0 \cdot 57$ nominal.

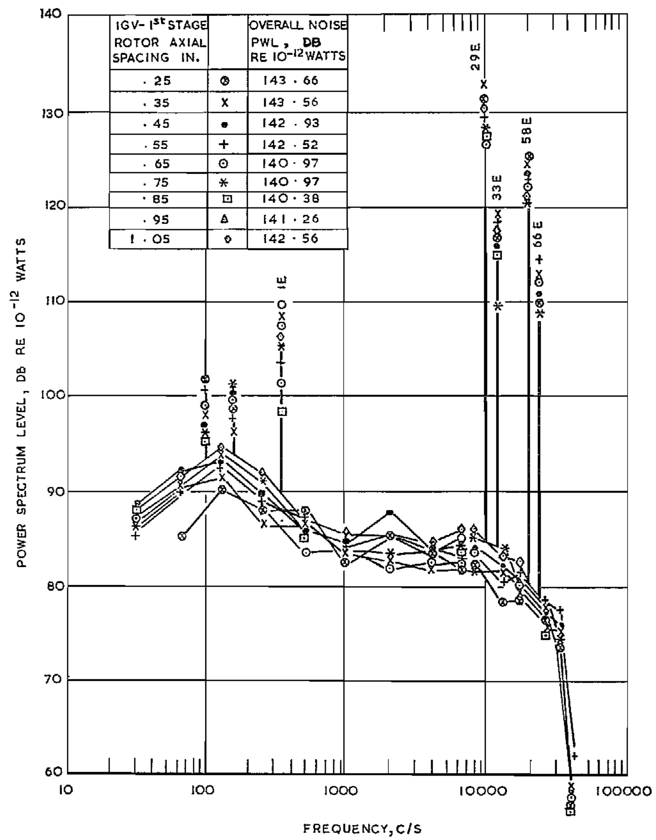

FIG. 18. Frequency spectrum—22 000 rev/min. $V_a/u = 0 \cdot 61$ nominal.

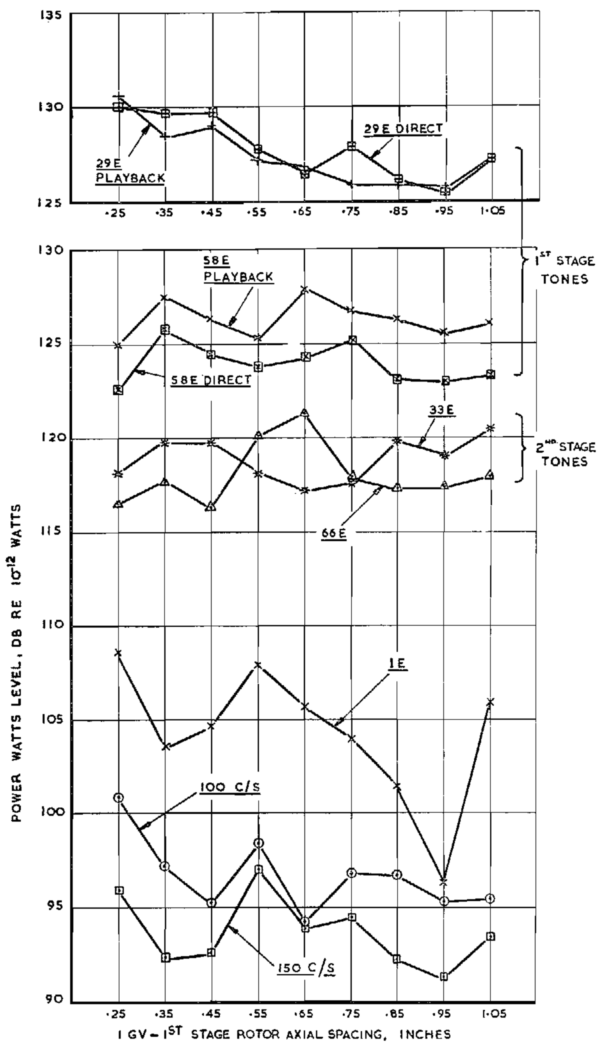

FIG. 19. Noise levels—18 000 rev/min. $V_a/u = 0 \cdot 57$ nominal.

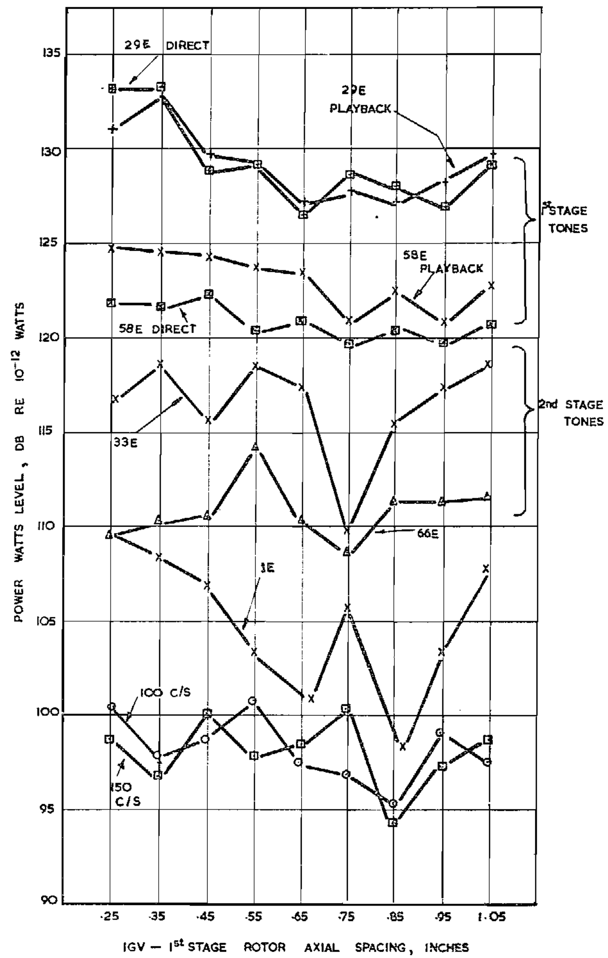

FIG. 20. Noise levels—22 000 rev/min. $V_a/u = 0 \cdot 61$ nominal.

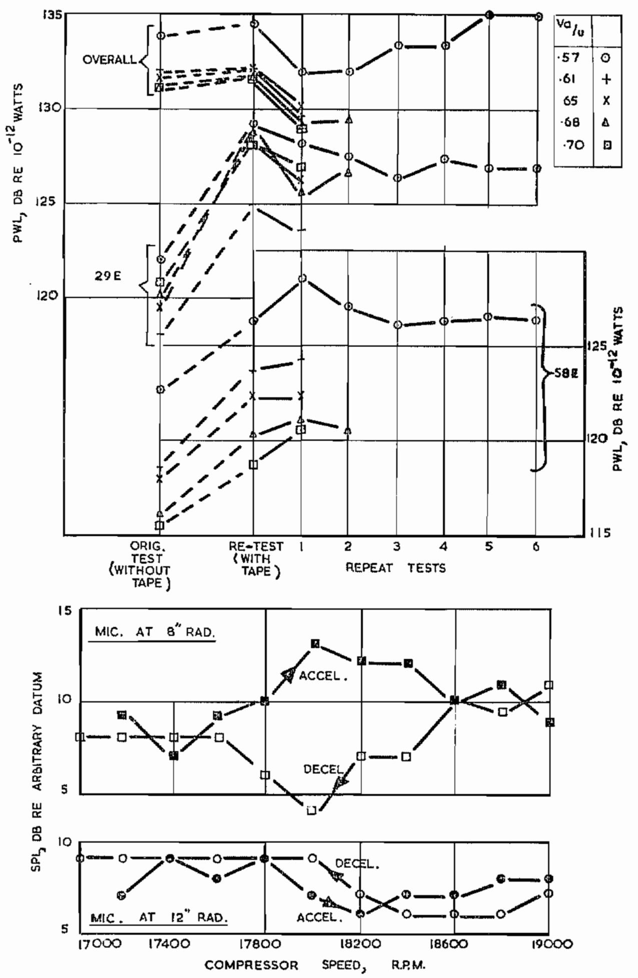

FIG. 21. An apparent anomaly. (I.G.V./rotor spacing 0·75; 18 000 rev/min.)

(91595) Wt. 66/3201 K.5 6/65 Hw.

Publications of the Aeronautical Research Council

ANNUAL TECHNICAL REPORTS OF THE AERONAUTICAL RESEARCH COUNCIL (BOUND VOLUMES)

1945 Vol. I. Aero and Hydrodynamics, Aerofoils. £6 10s. (£6 13s. 6d.)
Vol. II. Aircraft, Airscrews, Controls. £6 10s. (£6 13s. 6d.)
Vol. III. Flutter and Vibration, Instruments, Miscellaneous, Parachutes, Plates and Panels, Propulsion. £6 10s. (£6 13s. 6d.)
Vol. IV. Stability, Structures, Wind Tunnels, Wind Tunnel Technique. £6 10s. (£6 13s. 3d.)

1946 Vol. I. Accidents, Aerodynamics, Aerofoils and Hydrofoils. £8 8s. (£8 11s. 9d.)
Vol. II. Airscrews, Cabin Cooling, Chemical Hazards, Controls, Flames, Flutter, Helicopters, Instruments and Instrumentation, Interference, Jets, Miscellaneous, Parachutes. £8 8s. (£8 11s. 3d.)
Vol. III. Performance, Propulsion, Seaplanes, Stability, Structures, Wind Tunnels. £8 8s. (£8 11s. 6d.)

1947 Vol. I. Aerodynamics, Aerofoils, Aircraft. £8 8s. (£8 11s. 9d.)
Vol. II. Airscrews and Rotors, Controls, Flutter, Materials, Miscellaneous, Parachutes, Propulsion, Seaplanes, Stability, Structures, Take-off and Landing. £8 8s. (£8 11s. 9d.)

1948 Vol. I. Aerodynamics, Aerofoils, Aircraft, Airscrews, Controls, Flutter and Vibration, Helicopters, Instruments, Propulsion, Seaplane, Stability, Structures, Wind Tunnels. £6 10s. (£6 13s. 3d.)
Vol. II. Aerodynamics, Aerofoils, Aircraft, Airscrews, Controls, Flutter and Vibration, Helicopters, Instruments, Propulsion, Seaplane, Stability, Structures, Wind Tunnels. £5 10s. (£5 13s. 3d.)

1949 Vol. I. Aerodynamics, Aerofoils. £5 10s. (£5 13s. 3d.)
Vol. II. Aircraft, Controls, Flutter and Vibration, Helicopters, Instruments, Materials, Seaplanes, Structures, Wind Tunnels. £5 10s. (£5 13s.)

1950 Vol. I. Aerodynamics, Aerofoils, Aircraft. £5 12s. 6d. (£5 16s.)
Vol. II. Apparatus, Flutter and Vibration, Meteorology, Panels, Performance, Rotorcraft, Seaplanes. £4 (£4 3s.)
Vol. III. Stability and Control, Structures, Thermodynamics, Visual Aids, Wind Tunnels. £4 (£4 2s. 9d.)

1951 Vol. I. Aerodynamics, Aerofoils. £6 10s. (£6 13s. 3d.)
Vol. II. Compressors and Turbines, Flutter, Instruments, Mathematics, Ropes, Rotorcraft, Stability and Control, Structures, Wind Tunnels. £5 10s. (£5 13s. 3d.)

1952 Vol. I. Aerodynamics, Aerofoils. £8 8s. (£8 11s. 3d.)
Vol. II. Aircraft, Bodies, Compressors, Controls, Equipment, Flutter and Oscillation, Rotorcraft, Seaplanes, Structures. £5 10s. (£5 13s.)

1953 Vol. I. Aerodynamics, Aerofoils and Wings, Aircraft, Compressors and Turbines, Controls. £6 (£6 3s. 3d.)
Vol. II. Flutter and Oscillation, Gusts, Helicopters, Performance, Seaplanes, Stability, Structures, Thermodynamics, Turbulence. £5 5s. (£5 8s. 3d.)

1954 Aero and Hydrodynamics, Aerofoils, Arrester gear, Compressors and Turbines, Flutter, Materials, Performance, Rotorcraft, Stability and Control, Structures. £7 7s. (£7 10s. 6d.)

Special Volumes

Vol. I. Aero and Hydrodynamics, Aerofoils, Controls, Flutter, Kites, Parachutes, Performance, Propulsion, Stability. £6 6s. (£6 9s.)
Vol. II. Aero and Hydrodynamics, Aerofoils, Airscrews, Controls, Flutter, Materials, Miscellaneous, Parachutes, Propulsion, Stability, Structures. £7 7s. (£7 10s.)
Vol. III. Aero and Hydrodynamics, Aerofoils, Airscrews, Controls, Flutter, Kites, Miscellaneous, Parachutes, Propulsion, Seaplanes, Stability, Structures, Test Equipment. £9 9s. (£9 12s. 9d.)

Reviews of the Aeronautical Research Council

1949–54 5s. (5s. 5d.)

Index to all Reports and Memoranda published in the Annual Technical Reports

1909–1947 R. & M. 2600 (out of print)

Indexes to the Reports and Memoranda of the Aeronautical Research Council

Between Nos. 2451–2549: R. & M. No. 2550 2s. 6d. (2s. 9d.); Between Nos. 2651–2749: R. & M. No. 2750 2s. 6d. (2s. 9d.); Between Nos. 2751–2849: R. & M. No. 2850 2s. 6d. (2s. 9d.); Between Nos. 2851–2949: R. & M. No. 2950 3s. (3s. 3d.); Between Nos. 2951–3049: R. & M. No. 3050 3s. 6d. (3s. 9d.); Between Nos. 3051–3149: R. & M. No. 3150 3s. 6d. (3s. 9d.); Between Nos. 3151–3249: R. & M. No. 3250 3s. 6d. (3s. 9d.); Between Nos. 3251–3349: R. & M. No. 3350 3s. 6d. (3s. 10d.)

Prices in brackets include postage

R. & M. No. 3412

Printed and published by
HER MAJESTY'S STATIONERY OFFICE

To be purchased from
York House, Kingsway, London W.C.2
423 Oxford Street, London W.1
13A Castle Street, Edinburgh 2
109 St. Mary Street, Cardiff
39 King Street, Manchester 2
50 Fairfax Street, Bristol 1
35 Smallbrook, Ringway, Birmingham 5
80 Chichester Street, Belfast 1
or through any bookseller

Printed in England

R. & M. No. 3412

S.O. Code No. 33-3412